Radiative electron capture by bare and H-like Si and Cl ions using the channeling technique and the associated solid-state effect

Lokesh C. Tribedi, V. Nanal, M.B. Kurup, K.G. Prasad, and P.N. Tandon
Tata Institute of Fundamental Research, Bombay 400 005, India
(Received 14 June 1994)

Fully stripped and hydrogenlike Si and Cl ions, in the energy range 2–5 MeV/amu and channeled through a 0.17-μm thick Si single crystal, were used to study the radiative electron capture (REC) into the K shell of the ions. The associated effects due to the solid medium of the target were also investigated from the energy and the derived cross section of the REC photons. The K-shell REC cross sections were found to fall on a universal curve when plotted against the adiabaticity parameter of the collision system. The measured energy shifts in the REC photon energy and the higher yield of REC photons using crystalline targets, as compared to the available gas-target data, are indicative of an "ion–solid-state effect" caused by the electron-wake potential. The magnitude of these effects is shown to increase with Z/v of an ion with charge Z and velocity v, and is in qualitative agreement with recent calculations. The REC cross sections are, however, observed to be slightly smaller than the theoretical estimates after taking into account the effects associated with the solid medium. The widths of the REC peaks are compared with the theoretical models. The results of the present investigation using Si and Cl ions are presented coherently along with our earlier data using lighter ions.

PACS number(s): 34.70.+e, 34.50.−s, 61.80.Mk

I. INTRODUCTION

Radiative electron capture (REC) is a recombination process in which a highly ionized moving ion captures a quasifree electron and emits a stabilizing photon. It was first observed in fast ion solid collisions by Schnopper *et al.* [1]. Over the years it has been the subject of intense experimental and theoretical investigations [2–17]. A detailed account of the REC process is required in the description of the electron capture in high-energy heavy-ion collisions, in order to understand the ion–solid-state effect [15–17] and several other areas related to astrophysics and accelerators. Very recently, the REC process has been employed to investigate the atomic structure of hydrogenic heavy ions [18]. From the variation of the REC photopeak energy with the velocity of the ions, the binding energy of the captured electron in the moving ion has been determined. The binding energy of bound states of such highly ionized atoms provides stringent tests for the QED corrections to atomic theories. The REC is the dominant electron capture process in a very high-velocity ion-atom collision. A detailed theoretical investigation of REC in a relativistic atomic collision has been made recently [19, 20].

Within the validity of the impulse approximation, the cross section for REC into the K shell of a swift bare ion (atomic number Z and velocity v) per free electron can be represented in a closed analytical form in terms of a single parameter κ and is given by [21, 22]

$$\sigma_{\mathrm{REC}} = 9.1 \left(\frac{\kappa^3}{1+\kappa^2}\right)^2 \frac{\exp(-4\kappa\cot^{-1}\kappa)}{1-\exp(-2\pi\kappa)} 10^{-21}\ \mathrm{cm}^2. \tag{1}$$

Here $\kappa = Z\alpha/\beta$ is the Sommerfeld parameter, α the fine structure constant, and $\beta = v/c$. This formula, originally given by Stobbe [21], does not include the quasibound nature of the electrons in a target. The effect of a quasifree bound electron on the REC cross section has been considered by Kleber and Jakubassa [3]. They have shown that the cross section is seen to be approximately the recombination cross section for a free electron as given by Eq. (1). This equation suggests that it is possible to compare all REC cross sections, in a generalized picture, for different projectile velocities using various ions in terms of the quantity κ. Indeed, Stöhlker *et al.* [14] have shown that most of the available data on K-shell REC cross sections for a wide variety of ions at various energies when plotted against η_K ($\eta_K = \kappa^{-2}$) lie on a smooth curve. For fully stripped ions η_K is the same as the adiabaticity parameter, i.e., the ratio of the kinetic energy of the electron in the projectile frame to the binding energy of the K shell of the atom. For H-like ions η_K was calculated using the screened charge $Z_{\mathrm{sc}} = (Z-0.3)$, i.e., $\eta_K = V^2/Z_{\mathrm{sc}}^2$ where $V = v/v_0$ and v_0 is the Bohr velocity. This universality in cross section representation which was shown to hold for η_K values between 0.2 and 2.0 [14] has recently been extended to higher values of η_K, up to 10, from REC studies involving a variety of light ions as projectiles impinging on crystalline targets [15] and gas targets [16].

REC processes can also be used as a sensitive probe to investigate effects associated with the quasifree electrons of the solid medium which are captured by the moving ion. Spindler *et al.* [6] have shown that the intensity profile in the peak region of REC distributions can be accounted for quantitatively on the basis of proper momentum distributions of target electrons. Additionally, REC should also be sensitive to electron density fluctuations, of the quasifree electrons, created by the passage of

a swift charged particle through the solid medium. These electron density fluctuations dynamically screen the moving ion and the effects associated with it have been known for quite some time [23–27]. Our earlier studies on REC using crystalline targets [15] in fact suggest a definite increase in the derived values of the REC cross sections when compared with the existing gas-target data [14] corresponding to the same value of the adiabaticity parameter η_K of the collision system. Furthermore, it has been recently reported [17] and also observed by us [15] that the REC photopeak energy is slightly lower than the expected value from simple considerations of the transition from the valence band of the solid to the hydrogenic state of the moving ion (see also Ref. [16]). Both these observations, originating from the differences in the physical nature of the target, are attributed to the ion solid interaction mediated by the quasibound electrons of the medium. Recent calculations [28, 29] predict the increase in the electron density in the vicinity of the moving ion, as well as the REC photon energy shifts, to be proportional to Z/v. More measurements using a variety of ion beams at various energies are, therefore, desirable to test the predictions of these calculations. We have, therefore, measured these quantities from REC studies using Si and Cl beams at different energies and presented these results coherently along with our earlier data using C, O, F, and S ions. We have made use of the heavy-ion channeling technique for these measurements as it offers two main advantages [7, 12, 30, 31]: (i) the inhibition of close collisions between the ion and the crystal atoms makes the REC process relatively more dominant as the target-inner-shell x-ray production is highly suppressed, and (ii) consequently, the incident charge state of the ion is nearly preserved. In a channeling environment, therefore, ions of well-defined charge states move in a sea of dense quasifree electrons, conditions that are ideal for REC studies themselves as well as to probe the associated ion–solid-state effect.

II. EXPERIMENTAL DETAILS

The details of the experimental setup have been described elsewhere [15] and hence only necessary details will be provided. Ion beams of ^{28}Si and ^{35}Cl in the energy range between 2 and 5 MeV/amu were obtained before the BARC-TIFR Pelletron accelerator at Bombay. A post accelerator carbon foil stripper was used to obtain hydrogenic and fully stripped ions from the primary beam [32]. The charge selected beam from the switching magnet was collimated using two adjustable beam defining slits kept 1 m apart and at a distance of nearly 1 m before the scattering chamber. Both slits were kept at an opening of 0.5×0.5 mm^2 to obtain a nearly parallel beam. The well collimated beam was then directed onto a 0.17-μm-thick Si single crystal mounted on a double-axis goniometer. The same crystal was used in the earlier experiment also. The entire target chamber along with the beam dump was used as a Faraday cup and the charge collected was used for the beam normalization. In addition, the scattered particles from a thin self-supporting Au foil, kept 15 cm downstream from the target, were registered in a Si surface barrier detector kept at 90° to the beam direction. This provided an independent beam normalization. Both of these procedures gave the same results to within about 5%. Two Si(Li) detectors placed outside the scattering chamber at 55° and 135° with respect to the beam direction detected the x-ray photons emitted from the collision system. Both detectors had 165-eV energy resolution at 5.9 keV. The detectors had a 25-μm-thick Be window and were isolated from the chamber vacuum using a 24-μm Mylar window. The efficiency of the Si(Li) detector, in the range of 1–20 keV, was measured using the proton-induced x-ray emission technique as well as the standard radioactive sources [33]. It was again measured in the present geometry using a well calibrated ^{241}Am source and was found to be in good agreement with the earlier measured value [33]. Suitable absorbers made of Mylar foils of accurately known thickness were kept in front of the detector to cut down the target and the projectile x rays. For Si beams having energy lower than 77 MeV (i.e., for REC photon energy less than $\sim$ 4 keV) no external absorbers were used. The total transmission through the absorbers and the Be window was 53–83% for REC photons from Si beams at different energies and about 75–85 % for Cl REC photons. At a few energies the data were collected with and without the external absorber in order to estimate the errors due to the absorption correction. The maximum error was estimated to be about 10%. Total counting rates on the x-ray detector did not exceed 30 counts/sec for Si beams while collecting data for REC photons in the aligned position of the crystal. In the case of Cl beams these rates were about 50–60 counts/sec.

The thin self-supporting Si single crystal of 0.17-μm thickness was prepared by chemical etching [34] of a 300-μm-thick Si single crystal [(100), n-type, device grade]. Its thickness was measured accurately from the energy loss of α particles emitted from the ^{241}Am source. The $\langle 100\rangle$ axis of the crystal was aligned by monitoring the target x rays. The movement of the goniometer was controlled remotely by stepper motors with the help of a PC based control system [35]. The beam spot on the crystal was changed from time to time to minimize effects due to radiation damage. The alignment of the crystal was checked every time either the beam or its energy was changed. The yield of Si K x rays under well aligned conditions was observed to be about 10% of that in random directions.

III. RESULTS

A. K-shell REC cross sections

The x-ray spectra obtained using Si and Cl ions in the region of the REC peak are shown in Fig. 1 for some projectile energies. The K-shell REC photon peak is well pronounced and stands out quite well above the general background which is very essential to determine the area under the peak reliably and accurately. Several procedures for estimating the background under the REC peak were tried in order to minimize systematic errors in the area determination. The uncertainties in the back-

ground subtraction contributed mostly to the error in the area determination, the statistical error being small. In the case of Cl ions the REC spectra were found to be very clean and free from any impurity contribution [see Figs. 1(a) and 1(b)]. A small Ca contaminant was seen in the x-ray spectra using Si ions (see Fig. 1) which did not interfere significantly in determining the area under the REC photopeak. However, at 112 and 99 MeV bombarding energy of Si ions the x rays from Ca were inside the REC peak. Its contribution was estimated from the spectra obtained at lower as well as higher bombarding energies of the Si beam and accordingly corrected. This introduces an additional error in the area determination of the Si REC peaks, amounting to a maximum of 15%. The errors in the REC peak determination are estimated to be about 10% for other cases. The total K-shell REC cross section was deduced from the measured differential cross sections assuming $\sin^2\theta_{\rm lab}$ angular distribution for the K-shell REC photons [36],

$$\frac{d\sigma}{d\Omega} = \frac{3}{8\pi}\sigma_{\rm REC}\sin^2\theta_{\rm lab}, \tag{2}$$

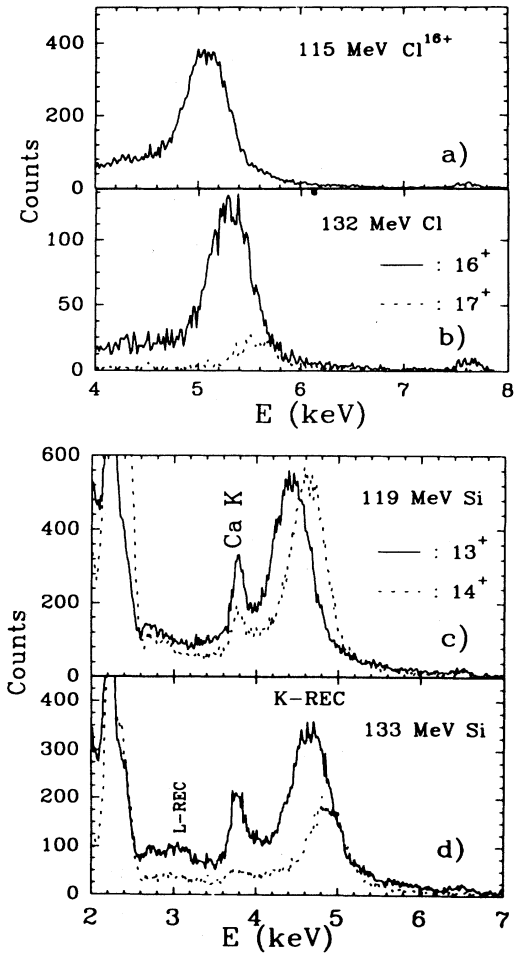

FIG. 1. Typical x-ray spectra showing the REC photopeak using Cl and Si ions. The spectra for bare (solid lines) and H-like (dashed lines) ions are not normalized to the same number of incident ions.

where

$$\frac{d\sigma}{d\Omega} = \frac{N_x}{\epsilon\phi_p N_e N_v}. \tag{3}$$

Here $\theta_{\rm lab}$ is the laboratory angle at which the REC photon is detected, N_x the number of counts under the REC photopeak, ϕ_p the number of incident particles, and ϵ the total efficiency of the x-ray detector, at a given photon energy, and includes the solid angle subtended by the target on the detector and the transmission factor of the external absorbers used. The quantity N_e is the total number of electrons sampled by the ions moving along the $\langle 100\rangle$ axis of the Si crystal and N_v the number of K-shell vacancies carried by the incident ions. Since all the cross-section data were collected using channeled ions the value of N_v was obtained from the respective incident K-shell vacancies assuming them to be frozen. Indeed the K-shell vacancies were found to be mostly frozen as was inferred from the relative intensities of the normal and hypersatellite components of the projectile x rays from hydrogenic and bare incident ions that have captured one electron [37].

To deduce the value of REC cross sections it is necessary to know the average electron density distribution along the $\langle 100\rangle$ axis. For Si the bulk electron density is 7×10^{23} cm^{-3}. Assuming only loosely bound electrons to contribute, one obtains 32 electrons per unit cell of Si to contribute to REC (Si has eight atoms per unit cell and four electrons in the M shell). Andriamonje *et al.* [12, 38] have calculated self-consistently the electron density distribution in a Si crystal along the $\langle 110\rangle$ axis to be 1.4×10^{23} cm^{-3} which corresponds to 22.4 electrons per unit cell. Datz *et al.* [39] have used a value of 1.44×10^{23} cm^{-3} for calculating atomic cross sections using channeled ions along the $\langle 110\rangle$ axis of a Si single crystal. We have earlier calculated [15] the electron density distribution along the $\langle 100\rangle$ axis of Si using the self-consistent field local density functional formalism and employing the embedded molecular cluster approach to simulate the bulk [40]. The electron density $\rho(\vec{r})$ was calculated [15, 41] using single-electron wave functions for solid silicon and the potential (U) was deduced from the electron density $\rho(\vec{r})$. Having obtained the electronic charge density $\rho(\vec{r})$ throughout the unit cell, the averaged electron density (ρ_u) along the $\langle 100\rangle$ axis per unit cell was obtained as

$$\rho_u = \frac{1}{a}\int_0^a \rho_{100}(z)dz, \tag{4}$$

where a is the lattice constant ($a = 5.432$ Å) and the z direction is taken along the $\langle 100\rangle$ axis. Figures 2(a) and 2(b) show the contour plots of ρ_u and the continuum potential U. The Si crystal has a diamond structure and the channel along the $\langle 100\rangle$ axis is constructed by the closest four atomic strings parallel to the $\langle 100\rangle$ direction and passing through the four corners of a square having dimension $\frac{1}{2\sqrt{2}}a$ where a is the lattice constant of Si. For ions moving in the center of the channel the electron density was calculated to be 1.68×10^{23} cm^{-3} [denoted by $\times$ in Fig. 2(b)] corresponding to 26.5 electrons per unit cell. Taking into account the divergence of beam (estimated

to be better than 1 mrad) in the present case, it was seen that all the channeled particles will be confined within the contour 2 [Fig. 2(a)] which is situated 0.33 Å away from the center of the channel or 1 Å away from the nearest atomic string. The maximum electron density sampled by the ions was estimated to be 1.8×10^{23} cm^{-3}, i.e., 29 electrons per unit cell. We have used the average electron density of 27.7 ± 1.3 electrons per unit cell for calculating the REC cross sections. As a check on the present calculations, we were also able to reproduce the continuum electron density along the ⟨110⟩ axis in Si as calculated in Ref. [42]. It is worth mentioning here that the channeled ions, considering their maximum divergence, lie within contour 2 [Fig. 2(b)] which is well outside the atomic L shell of Si. The L-shell electrons of the target are, therefore, not expected to contribute to the REC. This shows that the contribution to REC in the case of channeled ions comes essentially from the quasifree outer-shell conduction electrons.

The derived values for the K-shell REC cross section per electron and per K-shell vacancy in the projectile are shown in Fig. 3(a) as a function of beam energy. The errors in the cross sections are estimated to be about 20% for Cl and about 25% for Si data. These errors include the uncertainties in the area determination, detector efficiency including absorption corrections, crystal thickness and in determining the electron density distribution. The values obtained from fully stripped (open symbols) as well as H-like ions (filled symbols) are shown in this figure. The agreement between the values obtained using bare and H-like projectiles is quite good. The lines in the figure represent the calculations using Eq. (1).

The ratio (R) of REC yields (normalized to per ion and per electron) for fully stripped and H-like ions at the same ion velocity are also shown in Figs. 3(b) and 3(c). On a purely statistical basis one expects a value of 2 for this ratio since fully stripped ions have 2 K-shell vacancies. However, small deviations are expected for several reasons. (i) The small difference in the binding energies for the fully stripped and H-like ions and hence in their η_K values, at the same ion velocity, would imply difference in the REC cross sections. This would result in a slightly higher value of the ratio (i.e., $R > 2$). Using Eq. (1) the value of R was found to be ~ 2.1 for Si, S, and Cl; ~ 2.3 for O and F, and ~ 2.4 for C ions. They were found to be constant within $\sim 3\%$ in the present energy range. (ii) Preservation of charge states may not be to the same extent in both cases. (iii) Furthermore, the electron den-

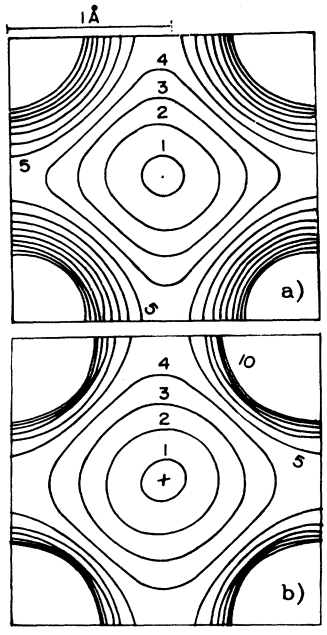

FIG. 2. (a) The map of the continuum potential averaged along the ⟨100⟩ direction of Si. The contours indicated by 1 to 13 correspond to 0.27, 1.36, 2.45, 3.54, 4.62, 5.71, 6.80, 7.89, 8.98, 10.06, 11.15, 12.24, and 13.32 eV. (b) The contour plots of the average electron density in a Si crystal averaged along the ⟨100⟩ direction. The contours indicated by 1 to 10 correspond to 0.168, 0.180, 0.193, 0.205, 0.218, 0.230, 0.243, 0.255, 0.268, and 0.280 $e/$Å^3.

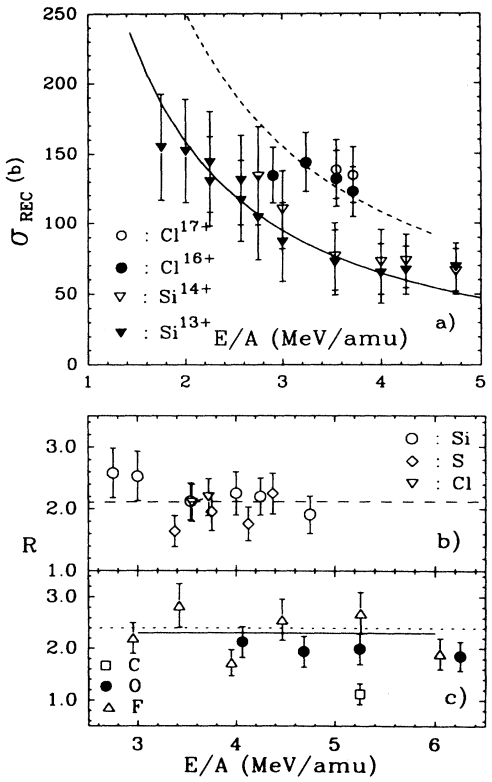

FIG. 3. (a) The total K-shell REC cross sections per electron per K vacancy as a function of energy per nucleon of the ions. The open (filled) symbols correspond to bare (H-like) ions. The solid and dashed lines correspond to the calculated values for Si and Cl ions, respectively, based on Eq. (1). The apparent good agreement with the theoretical calculations is because of the solid–state effect (see text for details, Sec. III). (b) The ratio R of the yields for bare to H-like ions of Si, S, and Cl as a function of energy of the ions. The dashed lines represent the expected ratio after correcting for the binding energy difference (see text). (c) The quantity R for C, O, and F ions. The solid line represents the expected values for O and F ions whereas the dotted line is for C ions.

sity sampled by the two types of ions may be slightly different. Though it is difficult to disentangle these effects, the overall agreement between the measured data and the calculated ratio for Si and Cl as well as S ions is very good, and thus signifying near preservation of initial charge states [see Fig. 3(b)]. We have also included in this figure [Fig. 3(c)] the ratio R for C, O, and F ions from our earlier measurements [15]. The agreement for O and F ions between the measured and the expected value is reasonably good. However, it can be seen that significantly large deviation is observed in the case of C ions [square in Fig. 3(c)]. This is attributed to a much larger fraction of fully stripped ions when H-like C ions are channeled. This observation is consistent with the recent results of Krause *et al.* [43] who have shown that in channeled conditions, depending on the ion energy, a majority of the H-like C ions come out as fully stripped.

B. Electron density enhancement

The universality of the REC cross sections would allow one to compare the data obtained for different projectiles having the same value of η_K. We have shown in Fig. 4 all

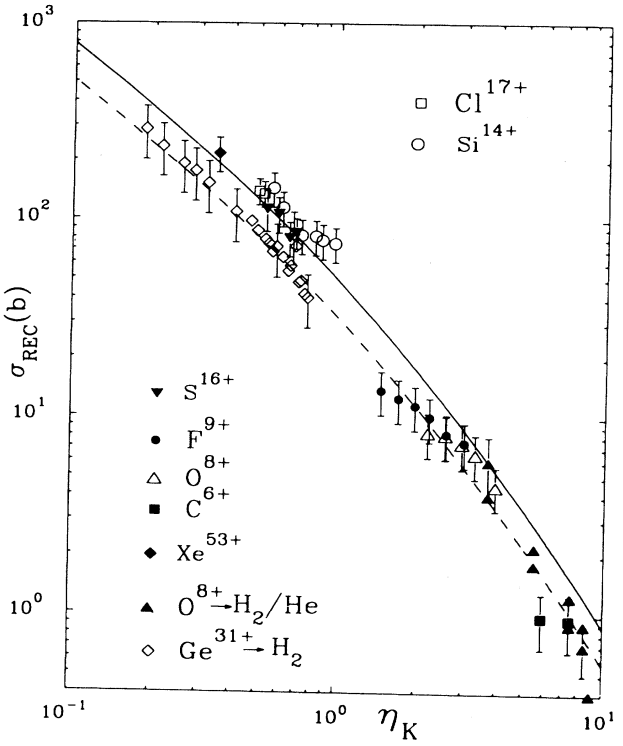

FIG. 4. The total K-shell REC cross section per electron per K vacancy as a function of the adiabaticity parameter η_K. The data for Si and Cl ions are from the present work. We have also included our earlier data for C, O, F, and S ions [15]. For clarity, we have included data using fully stripped ions only. The data of Ge on H_2 (open diamond), and Xe on Si (channeling; filled diamond) and O on He-H_2 (filled triangles) are taken from Refs. [14], [12], and [16], respectively. Errors are not shown on all points for better visualization. The solid lines represent the calculations using Eq. (1) and the dashed line is 35% below these calculations.

the recently available data on K-shell REC cross sections including the present work. The earlier data are taken from Refs. [12, 14–16]. We have included our earlier data for only fully stripped ions in order to avoid too much clustering of data points. The solid line represents the curve obtained using Eq. (1). Most of the data points corresponding to gas targets lie systematically below the theoretical curve, an observation made by earlier workers [14–16]. In the case of cross-section values derived using crystalline targets the data points corresponding to heavy ions ($Z \geq 14$) fall directly on the curve while most data points using lighter ions ($Z \leq 9$) fall below this curve. In fact, all the gas-target data and light-ion channeling data fall on the dashed line (Fig. 4) which is drawn 35% below the theoretical curve (solid line in Fig. 4). For a better visualization, at similar η_K values for the different collision systems we have shown in Fig. 5(a) the REC cross sections for heavy ions $Z \geq 14$ derived using crystal channeling [12, 15] and gas [14] targets including our present measurements with Si and Cl ions. Although the deviations, considering the errors on the data points, are statistically not very significant, the systematic difference between the gas-target data and the crystalline-target data is very obvious. In fact, the cross-section values derived using solid targets are about 50–100 % larger than those derived from gas targets at the corresponding values of η_K. This difference would further increase if one corrects for about 10–15 % of the incident ions which do not preserve their incident charge state in the channeled conditions. The present data lend further support to our earlier observation that there exists a difference in the derived values for the REC cross sections depending on the physical state of the target. This is in qualitative agreement with the expected increase in the electron density in the vicinity of the projectile in a solid medium [28, 29].

Figure 5(b) also shows a comparison of our crystalline-target data on lighter ions corresponding to higher values of η_K with that of a very recent measurement of Vane *et al.* [16] who have reported the REC cross-section data for oxygen ions using hydrogen and helium gas targets. The agreement between these two sets of data is quite good, suggesting the gas-solid state differences to be small for light ions (see also Fig. 4) in agreement with the theoretical expectations [28, 29]. It is desirable to have REC cross-section data using gas targets for η_K values varying between ~ 0.8 and 4. Such measurements are in progress using very heavy ions such as Pb and Au. Preliminary results of Stöhlker *et al.* [44] are consistent with the above observations.

C. Energy shifts of REC photons

Small energy shifts in the REC photopeak energy, as compared to theoretical estimates, have been reported recently [15, 17]. These shifts, observed only in solid medium [15, 17], are attributed to the ion–solid-state effect. We have also observed in the present studies, involving Si and Cl ions, that the REC peak lies below the theoretically expected values. These shifts were obtained reliably from the carefully recorded spectra with low count rates and calibrating the detector several times

before, during, and after the measurement using radioactive sources of ^{241}Am, ^{55}Fe, ^{57}Co, and Al K fluorescence x rays. There was no noticeable change in the calibration of the detectors. Typical values for the Doppler shifts of REC photons vary between 130 eV and 350 eV for 49–133-MeV Si beams. The uncertainties in the energy shifts were between 20–30 eV and arose mainly from peak fitting procedures. The expected energy for the REC photons was calculated using the following expression:

$$E_{\mathrm{REC}} = E_B + mc^2(\gamma - 1), \tag{5}$$

where m is the electron mass, and E_B is the binding energy of the K-shell electrons of the fully stripped or H-like ions. The REC photopeak energy in the projectile frame E_{REC} gets Doppler shifted in the laboratory frame according to

$$E_{\mathrm{REC}}^{\mathrm{lab}} = E_{\mathrm{REC}}\gamma^{-1}\left(1 - \beta\cos\theta_{\mathrm{lab}}\right)^{-1}. \tag{6}$$

The binding energy for the H-like ions was taken to be

$$E_B = 13.6Z^2, \tag{7}$$

and that for the He-like ions was obtained from the relation [11]

$$E_B(\mathrm{He}) - E_B(\mathrm{H}) = 0.315 - \tfrac{5}{4}Z\mathcal{R}_y \tag{8}$$

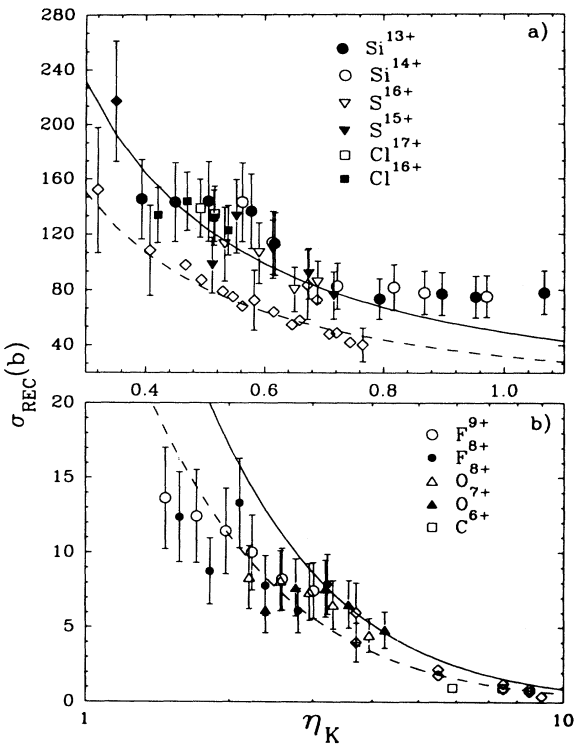

FIG. 5. The total K-shell REC cross sections for ions with (a) $Z \geq 14$ and (b) $Z \leq 9$ as a function of the adiabaticity parameter η_K. The solid lines represent calculations based on Eq. (1) and the dashed line is 35% below these calculations. The open diamonds in both panels represent the existing gas-target data which correspond to $Ge^{31+} \rightarrow H_2$ [14] in (a) and $O^{8+} \rightarrow H_2/He$ [16] in (b). The filled diamond is taken from Ref. [12].

where $\mathcal{R} = 1$ Ry. The shifts are found to vary between 40 and 80 eV [see Fig. 6(a)] and are well beyond the measuring accuracy. The agreement between the Doppler corrected photopeak energies measured in the two detectors, mounted at widely different angles of 55° and 135° is quite good, signifying that systematic errors are small.

D. REC x-ray width

The width of the REC x-ray peak originates from the initial momentum distribution of the target electrons that are captured. In the present case, the electrons contributing to the REC process are the loosely bound outer-shell electrons of Si. The widths of the REC photopeaks deduced from the Gaussian fits to the data, after correcting for the detector resolution, are shown in Fig. 7. In this figure the widths of Cl, S, and Si REC peaks are plotted as a function of the ion velocity. For Si ions the

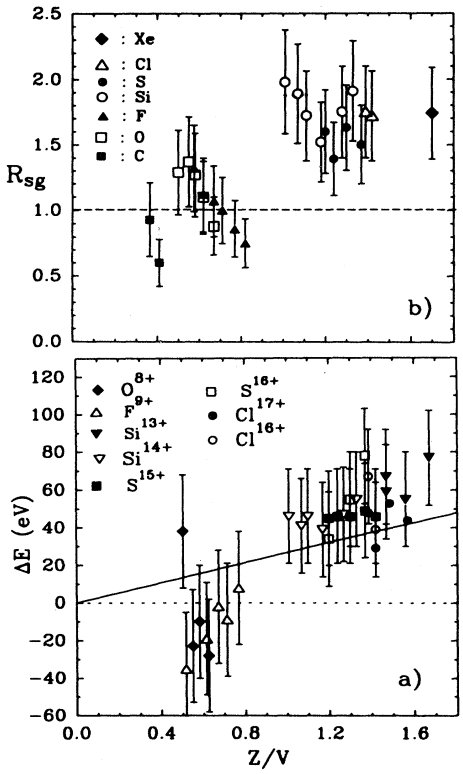

FIG. 6. (a) The energy shift in the REC photopeak ΔE as a function of Z/V of the ion for Si and Cl ions. We have also included the data of C, O, F, and S ions from our earlier measurements [15]. The solid line is based on the calculations by Pitarke *et al.* [29] which include the wake potential contribution to the energy shifts. (b) The ratio (R_{sg}) of the REC cross sections obtained using crystalline targets to those obtained by using gas targets [14,16] as a function of Z/V of the ions. For gas-target data the dashed line of Fig. 4 is used (see text for details). The filled diamond was deduced using the data for Xe ions from Ref. [12]. The data of C, O, F, and S ions are taken from our earlier work [15]. For lighter projectiles ($Z \leq 17$) the REC cross sections are used only for the fully stripped ions to deduce R_{sg}.

widths are shown at those velocities for which the REC peak is free from the Ca contamination.

In a simple picture the REC peak width can be viewed as the Doppler broadening [3], i.e., the energy of the photon emitted depends on the z component (parallel to v) of the electronic momentum in the initial state. Then the full width at half maximum (FWHM) of the REC photopeak δE, can be written as [3, 9]

$$\delta E = 2vp_{iz} = 2\left[4(m/M)E_1\epsilon_i\right]^{1/2}, \tag{9}$$

where ϵ_i is the average binding energy of the M-shell electrons of the Si atom, m and M are the mass of electron and the projectile, respectively. The factor 2 is due to the two directions of p_{iz}. The widths derived using this formula are shown in Fig. 7 by a dashed line which reproduced the data quite well. It can be mentioned here that using the Fermi energy of Si solid for ϵ_i one obtains the widths that are slightly (~4%) less compared to the dashed line.

Since the energy distribution of REC photons depends on the momentum distribution of the target electrons to be captured, the REC peak shape should depend on the Compton profile $I(p_{iz})$ of these electrons. This quantity represents the probability of finding the electron with momentum p_{iz}. For a H-like atom it can be written as [3]

$$I_i(p_{iz}) = \frac{8\alpha_i^5}{3\pi(p_{iz}^2+\alpha_i^2)^3}\ , \tag{10}$$

where $\alpha_i = Z_2^{sc}m^2/\hbar n$ and Z_2^{sc} is the screened nuclear charge of the Si atom as seen by the outermost electrons. The FWHM (W) of such a profile can be written to a very good approximation [3] as $W \approx v\alpha_i$. This quantity is shown by a solid line in Fig. 7. The agreement between the calculated values and the observed data is reasonably good. This was also observed by Tawara *et al.* [9] for F ions on a He target, and recently by Vane *et al.* [16] using oxygen ions on H_2 and He targets. The widths measured for the same velocity Si, S, and Cl ions as well as those for the H-like and bare ions are found to be the same within the measuring accuracy. These are consistent with the fact that the REC widths at a given ion velocity will only depend on the momentum distribution of the target electrons, not on the atomic number or the charge states of these ions. As discussed before, the bare and H-like ions having different screened charge and hence with slightly different transverse energies may sample the quasifree electrons with slightly different Compton profiles. This effect may provide a slight difference in the corresponding REC widths which are, however, within the uncertainties shown in the figure.

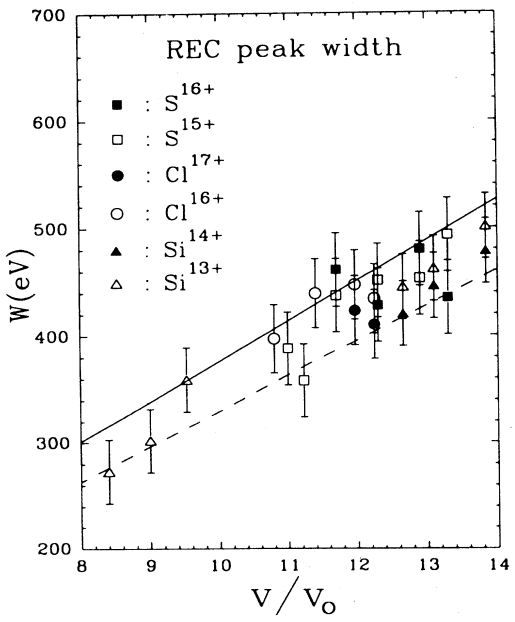

FIG. 7. The width of the REC photopeak as a function of the velocity of the ion. The dashed line is obtained using Eq. (9) and the solid line using Eq. (10). For details see text.

IV. DISCUSSIONS

A. Solid-state effect

It is known that when a fast charged particle moves through a solid, polarization of the medium occurs which leads to dynamical screening by the electron gas through a wake potential. The electrons bound to the ion are affected by this screening. The enhancement of the mean electron density of the polarized medium, which occurs in the vicinity of the projectile, induces a potential at the site of the projectile and is given in the linear approximation by [28, 29]

$$\lim_{r\to 0}\left[\phi(r)-\frac{Z}{r}\right] = -\frac{\pi Z\omega_p}{2}\ , \tag{11}$$

where $\phi(r)$ is the total wake potential of the projectile moving in the medium and ω_p is the plasma frequency. Consequently, the energy eigenvalue for the lowest state of the hydrogenlike moving ion E_f should be

$$E_f = -\frac{1}{2}\mathcal{R}Z^2 + \frac{\pi Z\omega_p}{2}. \tag{12}$$

Furthermore, using the appropriate form for the dielectric function, it has been shown [28, 29] that the electron density (ρ) is enhanced at the ion by the amount

$$\delta\rho \simeq \frac{Z}{V}\rho\pi\ , \tag{13}$$

where V is in atomic units. It may be noted that the energy shift and the density enhancement in a given medium are proportional to Z/v.

We have shown in Fig. 6(a) the energy shifts observed for the REC x rays for Si and Cl ions as a function of Z/V of the ion along with our earlier results [15]. For light ions, the results of which are taken from our earlier published work [15], most data points fall below the zero line indicating a small systematic error arising mostly due to the shape of the bremsstrahlung background spectra under the REC peak. For heavier ions, because of larger REC cross sections and smaller contributions due to bremsstrahlung this systematic error is negligible.

Even though the energy shifts observed using lighter ions are small and consistent with zero within the measuring accuracy, nevertheless, they have also been included to establish the increasing trends in the Z/v dependence of these shifts. The data points span a region of 0.4 to 1.7 in Z/V. It is apparent that the shifts tend to increase with Z/v of the ion. Pitarke *et al.* [29] have calculated the shift in the REC peak for bare S ions in the energy range 100–200 MeV channeled in a Si single crystal using a statistical local density approach. The calculations have been made when the minimum impact parameter is taken to be 0.1 Å. The contribution to REC peak shift, coming from the wake correction to the binding energy of the captured electron [see Eq. (8)] in the case of S ions is shown in the figure by a solid line (see Ref. [29]). The calculated values lie systematically below the data points for Si, S, and Cl ions. The calculation can explain a shift of about 40–50 eV for S ions invoking the wake effect. According to Pitarke *et al.* [29] the rest of the shift ($\sim$ 30–40 eV) could be explained by assuming a substantial amount of electrons being captured from the L shell in a low impact parameter ($\sim$ 0.1 Å) collision which is not a valid assumption in the present case as discussed in Sec. III A.

The differences in the REC cross-section values between gas and solid targets are larger for heavier ions ($Z \geq 14$) as compared to light ions $Z \leq 9$ (see Fig. 5). This is more apparent from Fig. 6(b) in which we have plotted, as a function of Z/V of the ion, the ratio of the derived value of the REC cross sections using solid targets with that using gas targets. Since the corresponding gas data are not available for all the solid target data, we have used a value which is 35% smaller than the theoretical value for the gas data. This is fully justified as most gas-target data for Ge and O ions for η_K values varying from 0.3 to 10 lie on this curve (see Fig. 4). The errors shown in the ratio reflect the errors in the solid target data. The scaling of the cross sections with Z/v of the ion is in agreement with Eq. (13). As seen from Fig. 6(b) the data points are clustered around two values of Z/V, 0.6 and 1.3, corresponding to the light and heavy ions, respectively. The average value of the ratio is close to unity for light ions while significant deviations are observed for heavy ions. On an average the enhancement in the REC cross section values observed is about 70% over that of gas targets. The maximum enhancement is shown to be a factor of 2 which is considerably smaller than the expected electron density enhancement as predicted by the theoretical consideration [see Eq. (13)]. The observed enhancement demonstrates the sensitivity of the REC process for probing such solid-state effects on the moving ions.

B. REC cross section

As has been discussed earlier, the K-shell REC cross sections using the gas-target data and the data using light channel ions, where one does not expect a significant ion–solid-state effect, fall on a universal curve (Fig. 4) that lies about 35% below the theoretical calculations [Eq. (1)]. Such deviations from theory were also suggested by us from our earlier studies [15] using C, O, and F ions and more recently by Vane *et al.* [16] using oxygen-ion data and by Stöhlker *et al.* [14] for Ge ions. These deviations may be attributed to the quasifree nature of the electrons captured. Detailed calculations are required to ascertain its validity for quasibound electrons.

It should be mentioned here that one also expects to see in the present measurements a REC photon peak corresponding to the capture in the L shell of the projectile. We did, however, see a small peak at the expected energy corresponding to the L-shell REC x ray for 133-MeV Si ions, which merged into the projectile x-ray peak at lower bombarding energies (see Fig. 1). The intensity of this peak was, however, below the expected intensity taking into account the loss of intensity due to absorption in external absorbers.

V. CONCLUSION

We have measured the cross sections for REC into the K shell of several bare and H-like projectiles at different energies using the channeling technique. All the REC cross sections are presented for comparison as a universal function of a scaled variable η_K. The cross-section values obtained in the present work using channeled ions when compared with the existing gas-target data suggest a solid-state effect that manifests itself as a dynamical screening of the ions due to the enhancement of electron density at the projectile site. The resulting wake potential acting on the ions could explain qualitatively the Z/v dependent shifts in the REC photopeak energies although the electron density enhancements are shown to be considerably smaller compared to the theoretical predictions [29]. The K-shell REC cross sections are found to be slightly smaller than the theoretical estimates [21, 22]. The REC x-ray widths can be understood in terms of the existing models.

ACKNOWLEDGMENTS

The authors thank J. Eichler for helpful discussions. They thank N. Bhattacharya, W.A. Fernandes, and D.C. Karve for their help during the measurements, P.R. Apte for his help in preparing the Si single crystal target, and the accelerator staff for smooth operation of the machine.

[1] H.W. Schnopper, Hans D. Betz, J.P. Delvaille, K. Kalata, A.R. Sohval, K.W. Jones, and H.E. Wegner, Phys. Rev. Lett. **29**, 898 (1972).

[2] P. Kienle, M. Kleber, B. Povh, R.M. Diamond, F.S. Stephens, E. Grosse, M.R. Maier, and D. Proetel, Phys. Rev. Lett. **31**, 1099 (1973).

[3] M. Kleber and D.H. Jakubassa, Nucl. Phys. **A252**, 152 (1975).

[4] R. Schule, H. Schmidt-Boecking, and I. Tserruya, J. Phys. B **10**, 889 (1977).

[5] J.A. Tanis and S.M. Shafroth, Phys. Rev. Lett. **40**, 1174 (1978).

[6] E. Spindler, H.D. Betz, and F. Bell, J. Phys. B **10**, L561 (1977).

[7] B.R. Appleton, R.H. Ritchie, J.A. Briggerstaff, T.S. Noggle, S. Datz, C.D. Moak, H. Verbeek, and V. Neelavathi, Phys. Rev. B **19**, 4347 (1979).
[8] J.A. Tanis, W.W. Jacobs, and S.M. Shafroth, Phys. Rev. A **22**, 483 (1980).
[9] H. Tawara, Patrick Richard, and K. Kawatsura, Phys. Rev. A **26**, 154 (1982).
[10] S.M. Shafroth, K. Shima, T. Ishihara, T. Mikumo, T. Miyoshi, T. Mamoi, M. Moriyama, H. Ohara, Y. Tagishi, H. Yamaguchi, and M. Yamanouchi, IEEE Trans. Nucl. Sci. **NS-30**, 1055 (1983).
[11] R. Anholt, Ch. Stoller, J.D. Molitoris, D.W. Spooner, E. Morenzoni, S.A. Andriamonje, W.E. Meyerhof, H. Bowman, J.S. Xu, Z.Z. Xu, J.O. Rasmussen, and D.H.H. Hoffmann, Phys. Rev. A **33**, 2270 (1986).
[12] S. Andriamonje, M. Chevalier, C. Cohen, J. Dural, M.J. Gaillard, R. Genre, M. Hage-Ali, R. Kirsch, A. L'Hoir, B. Mazuy, J. Mory, J. Moulin, J.C. Poizat, J. Remillieux, D. Schmaus, and M. Toulemonde, Phys. Rev. Lett. **59**, 2271 (1987).
[13] K. Kawatsura, A. Ootuka, M. Sataka, K. Komaki, H. Naramoto, K. Ozawa, Y. Nakai, and F. Fujimoto, Nucl. Instrum. Methods Phys. Res. Sect. A **262**, 33 (1987).
[14] Th. Stöhlker, C. Kozhuharov, A.E. Livingston, P.H. Mokler, Z. Stachura, and A. Warczak, Z. Phys. D **23**, 121 (1992).
[15] L.C. Tribedi, V. Nanal, M.R. Press, M.B. Kurup, K.G. Prasad, and P.N. Tandon, Phys. Rev. A **49**, 374 (1994).
[16] C.R. Vane, S. Datz, P.F. Dittner, J. Giese, N.L. Jones, H.F. Krause, T.M. Rosseel, and R.S. Peterson, Phys. Rev. A **49**, 1847 (1994).
[17] C.R. Vane, P.F. Dittner, H.F. Krause, J. Gomes del Campo, N.L. Jones, P.A. Zeijimans Von Emmichoven, U. Bechthold, and S. Datz, Nucl. Instrum. Methods Phys. Res. Sect. B **67**, 256 (1992).
[18] P.H. Mokler, Th. Stöhlker, C. Kozhuharov, Z. Stachura, and A. Warczak, Z. Phys. D **21**, 197 (1991).
[19] J. Eichler, Phys. Rep. **193**, 165 (1990).
[20] A. Ichihara, T. Shirai, and J. Eichler, Phys. Rev. A **49**, 1875 (1994).
[21] M. Stobbe, Ann. Phys. (Leipzig) **7**, 661 (1930).
[22] H.A. Bethe and L.E. Salpeter, *Quantum Mechanics of One and Two Electron Atoms* (Academic Press, New York, 1957), p. 320.
[23] W. Brandt, A. Ratkowski, and R.H. Ritchie, Phys. Rev. Lett. **33**, 1329 (1974); **35**, 130(E) (1975).
[24] D.S. Gemmell, J. Remillieux, M.J. Gaillard, R.E. Holland, and Z. Vager, Phys. Rev. Lett. **34**, 1420 (1975).
[25] R. Laubert and F.K. Chen, Phys. Rev. Lett. **40**, 174 (1978).
[26] S. Datz, C.D. Moak, O.H. Crawford, H.F. Krause, P.F. Dittner, J. Gomez del Campo, J.A. Biggerstaff, P.D. Miller, P.V. Hvelplund, and H. Knudsen, Phys. Rev. Lett. **40**, 843 (1978).
[27] F. Bell, H.D. Betz, H. Panke, and W. Stehling, J. Phys. B **9**, L443 (1976).
[28] P.M. Echenique, R.H. Ritchie, and W. Brandt, Phys. Rev. B **20**, 2567 (1979).
[29] J.M. Pitarke, R.H. Ritchie, and P.M. Echenique, Phys. Rev. B **43**, 62 (1991); J. Burgdorfer, Nucl. Instrum. Methods Phys. Res. B **67**, 1 (1992).
[30] N. Claytor, B. Feinberg, H. Gould, C.E. Bemis, Jr., J. Gomez del Campo, C.A. Ludemann, and C.R. Vane, Phys. Rev. Lett. **61**, 2081 (1988).
[31] A. Belkacem, E.P. Kanter, K.E. Rehm, E.M. Bernstein, M.W. Clark, S.M. Ferguson, J.A. Tanis, K.H. Berkner, and D. Schneider, Phys. Rev. Lett. **64**, 380 (1990).
[32] S.D. Narvekar, R.R. Hosangadi, L.C. Tribedi, R.G. Pillay, K.G. Prasad, and P.N. Tandon, Pramana **39**, 79 (1992).
[33] L.C. Tribedi and P.N. Tandon, Nucl. Instrum. Methods Phys. Res. Sect. B **62**, 178 (1992).
[34] Vandana Nanal, P.R. Apte, M.B. Kurup, and K.G. Prasad, Nucl. Instrum. Methods Phys. Res. Sect. B **82**, 404 (1993).
[35] Vandana Nanal, W. Fernandes, M.B. Kurup and K.G. Prasad, Nucl. Instrum. Methods Phys. Res. Sect. B **73**, 101 (1993).
[36] E. Spindler, H.D. Betz, and F. Bell, Phys. Rev. Lett. **42**, 832 (1979).
[37] L.C. Tribedi, Ph.D. thesis, University of Bombay, 1993 (unpublished)
[38] S. Andriamonje, M. Chevalier, C. Cohen, J. Dural, M.J. Gaillard, R. Genre, M. Hage-Ali, R. Kirsch, A. L'Hoir, B. Kazuy, J. Mory, J. Moulin, J.C. Poizat, J. Remillieux, D. Schmaus, and M. Toulemonde, J. Phys. (Paris) Colloq. **C-50**, 285 (1989).
[39] S. Datz, P.F. Dittner, J. Gomez del Campo, H.F. Krause, T.M. Rosseel, and C.R. Vane, Z. Phys. D **21**, S45 (1991).
[40] D.E. Ellis, G.A. Benes, and E. Byrom, Phys. Rev. B **16**, 3308 (1977), and references therein.
[41] M.R. Press (private communication).
[42] A. L'Hoir, S. Andriamonje, R. Anne, N.V. de Castro Faria, M. Chevalier, C. Cohen, J. Dural, M.J. Gaillard, R. Genre, M. Hage-Ali, R. Kirsch, B. Farizon-Mazuy, J. Mory, J. Moulin, J.C. Poizat, Y. Quere, and J. Remilleux, Nucl. Instrum. Methods Phys. Res. Sect. B **48**, 145 (1990).
[43] M.F. Krause, J.H. Barrett, S. Datz, P.F. Dittner, N.L. Jones, J. Gomez del Campo, and C.R. Vane, Phys. Rev. A **49**, 283 (1994).
[44] Th. Stöhlker, F. Bosch, B. Franzke, M. Zung, O. Klepper, P.H. Mokler, R. Moshammer, and H. Reich, GSI Report 93-1 b 185 (1992) (unpublished).